PHILOSOPHICAL TRANSACTIONS OF THE ROYAL SOCIETY A MATHEMATICAL, PHYSICAL & ENGINEERING SCIENCES

Liquid Crystal Phases of Self-Assembled Amphiphilic Aggregates

Thomas L. Madden and Judith Herzfeld

Phil. Trans. R. Soc. Lond. A 1993 **344**, 357-375
doi: 10.1098/rsta.1993.0095

Liquid crystal phases of self-assembled amphiphilic aggregates

By Thomas L. Madden and Judith Herzfeld

Department of Chemistry, Brandeis University, Waltham, Massachusetts 02254-9110, U.S.A.

Long-range order in solutions of reversibly self-assembling molecules results from interactions among the asymmetric aggregates. Even for electrically neutral species, repulsions between the aggregates become significant at high concentrations. At the very least, the excluded volume of asymmetric aggregates creates formidable packing constraints which are relieved by orientational and positional alignment. Aggregate growth thus promotes long-range order, and long-range order facilitates growth. Nematic phases occur if aggregate growth is strong enough to induce orientational ordering at concentrations lower than those that induce positional ordering. The symmetry of the positionally ordered phases reflects aggregate morphology: the polydispersity of aggregates that grow in one (two) dimension(s) to form rod-like (plate-like) particles suppresses the smectic (columnar) phase in favour of the columnar (smectic) phase. Because plate-like aggregates pack more easily than rod-like aggregates, increasing concentration induces a rearrangement from rod-like to plate-like aggregates, and a transition from columnar to smectic ordering, in solutions of molecules, such as surfactants, capable of forming both types of aggregates. In mixtures of aggregating and non-aggregating species, the difficulty of packing spherically shaped particles among elongated particles results in dramatic demixing such that a very concentrated solution of very large, highly aligned aggregates coexists with a relatively dilute solution depleted of the aggregating species.

1. Introduction

Aggregates of amphiphilic molecules can be highly asymmetric. For example, consider a simple binary solution of a surfactant in water. As the concentration of surfactant increases, the molecules form micelles which sequester the hydrophobic parts of the molecules from the water, while leaving the hydrophilic parts exposed. Although the smallest micelles are approximately spherical, micelles can grow by addition of monomers to form cylindrical or discoidal aggregates (Tanford 1973). This reversible process generally produces a highly polydisperse population of asymmetric particles.

The asymmetry of grown out micelles leads to long-range order at high concentrations, analogous to that seen in monodisperse lyotropic liquid crystals. As the concentration increases, there is an orientational ordering transition which is driven by a concomitant gain in translational freedom (Onsager 1949). There can also be translational ordering in some dimensions driven by a gain in translational

Phil. Trans. R. Soc. Lond. A (1993) **344**, 357–375
Printed in Great Britain

freedom in other dimensions (Taylor *et al.* 1989*b*). The orientational ordering transition is qualitatively the same for polydisperse particles as for monodisperse particles. The positional ordering transition, on the other hand, is very sensitive to end or edge effects: polydispersity destabilizes the smectic phase of cylindrical aggregates and the columnar phase of discoidal aggregates.

The long-range order arising from particle asymmetry in reversibly assembling systems differs from that in other systems of polydisperse asymmetric particles in that there is a reciprocal effect of long-range order on particle asymmetry: by relieving packing constraints, long-range order promotes aggregate growth. The particle size distribution is thus coupled to the orientation and position distributions and any theoretical description of the phase behaviour must take the joint optimization of these many degrees of freedom into account (Herzfeld & Briehl 1981; McMullen *et al.* 1985).

2. Free energy and the equilibrium distribution of aggregate sizes, orientations and positions

In describing the liquid crystalline behaviour of reversibly assembling systems we are concerned with length scales on the order of the dimensions of the aggregates and are not concerned with the internal structure of the aggregates. The states of the system can therefore be adequately described by the number concentration, $c(n, \Omega)$, of particles with aggregation number, n, and orientation, Ω. As described below, particle positions are assumed to be random within the constraints appropriate for each phase (i.e. restriction to cells for the crystalline phase, restriction to tubes for the columnar phase, restriction to layers for the smectic phase, and no restriction at all for the nematic and isotropic phases) (Taylor *et al.* 1989*a*). The partition function is then the sum over all possible distributions $c(n, \Omega)$ of the function

$$\{g(c(n, \Omega)) \exp[-E(c(n, \Omega))]\},$$

where $g(c(n, \Omega))$ and $E(c(n, \Omega))$ are the degeneracy and the energy of the state $c(n, \Omega)$ respectively. The degeneracy of the state takes into account the degrees of freedom internal to the aggregates, the permutations available in mixing aggregates of different sizes and orientations, the particle positions available without violating excluded volume, and the degrees of freedom of the solvent. The energy of the state takes into account the energy of the aggregates and the solvent, including all interactions within and between the solute and solvent molecules. If we approximate the partition function by its maximum term, then the equilibrium state $c(n, \Omega)$ is the one that minimizes the free energy functional $F(c(n, \Omega)) = -\ln g(c(n, \Omega)) + E(c(n, \Omega))$. The theoretical problem then reduces to deriving an appropriate expression for $F(c(n, \Omega))$. For this purpose it is convenient to consider $f = \beta F/V$, the free energy per unit volume in units of kT.

There are three contributions to the free energy:

$$f = f_{\text{assoc}} + f_{\text{mix}} + f_{\text{inter}}. \tag{2.1}$$

The contribution due to the association of monomers to form aggregates includes the free energy changes involved in forming contacts between monomers. This term tends to favour aggregate growth. The free energy of mixing favours the disordering

of aggregates and dissociation into monomers. The non-ideal contribution, due to interactions between aggregates, includes hard core and soft repulsions. The hard core interactions favour long-range order at high concentrations, as discussed above. Soft repulsions, on the other hand, oppose parallel orientations. In the remainder of this section we consider the various ways in which these three free energy terms have been treated.

(*a*) *The free energy of association*

As we are not concerned with the details of the internal structure of the aggregates, the free energy of association can be treated phenomenologically with just one parameter for each structurally distinct form of aggregation. The simplest case is isodesmic association in which each additional monomer forms contacts with the same free energy. In this case,

$$f_{\text{assoc}} = -\phi \int c(n, \Omega)\,(n-1)\,\mathrm{d}n\,\mathrm{d}\Omega, \tag{2.2}$$

where ϕ is the free energy of each contact in units of kT. This corresponds to linear aggregation (in which monomers stack to form cylindrical aggregates of the same width) and provides a good description of the association of polyaromatic dyes and drugs (Taylor & Herzfeld 1990, 1991*a*).

For nonlinear aggregates, it is necessary to take into account the different environments of different monomers. For thick rod-like aggregates, there are monomers on the ends that are missing some stabilizing contacts compared to the monomers in the rest of the aggregate. A minimal description of this situation treats the ends of an aggregate as two halves of a minimum aggregate, with an average free energy of contacts per monomers of ϕ_0. The rest of the monomers in the middle of the extended aggregate each contribute an average of ϕ_1 to the free energy of association. This type of formalism has been used to model the formation of multistranded fibres by self-assembling proteins (Herzfeld 1988; Herzfeld & Taylor 1988; Hentschke & Herzfeld 1989*a*, *b*, 1991). By adjusting the two ϕs it is possible to model the cooperativity of assembly.

Surfactants also form nonlinear aggregates and cylindrical micelles can be treated in the same way as the protein aggregates. McMullen *et al.* (1984*b*) emphasize that the free energy of association per surfactant monomer depends on the surface area per hydrophilic head group and the internal packing of the hydrophobic tail. Since the curvature of a spherocylindrical micelle is different in the hemispherical endcaps than in the cylindrical middle section, the free energy of association per monomer is different. Such a treatment can be extended to discoidal micelles by introducing another parameter, ϕ_2, for the average free energy of monomer contacts in the flat portion of the micelle (Taylor *et al.* 1989*a*).

(*b*) *The free energy of mixing*

The free energy of mixing has the form

$$f_{\text{mix}} = \int c(n, \Omega)\,[\ln\,(c(n, \Omega)\,\lambda^3) - 1]\,\mathrm{d}n\,\mathrm{d}\Omega, \tag{2.3}$$

where λ is a length scale which may be derived from the single particle partition function. The n-dependence of the single particle partition function can also be

included explicitly (McMullen *et al.* 1984*a*; Hentschke & Herzfeld 1991; Taylor & Herzfeld 1991*a*). However, the n-dependence of the rotational and translational parts is weak and does not qualitatively affect the phase behaviour. The n-dependence of the vibrational part is stronger but more difficult to evaluate and, in any case, can be absorbed into the solute chemical potential (see χ in §2*d*).

(*c*) *Free energy of interparticle interactions*

Treatments of interactions between particles in lyotropic systems usually take the solvent as background, so that interactions between two particles are referenced to the interactions that would otherwise occur between the particles and solvent (see, for example, Onsager 1949). This avoids the need for an explicit description of solvent–solvent and solvent–particle interactions, both of which are still problematic for a solvent as complicated as water.

Interactions between particles may include long-range electrostatic forces and short-range soft repulsions or attractions, as well as the hard-core excluded volume interactions. Here we will be concerned exclusively with hard core excluded volume and weak short-range interactions. The results will therefore apply to uncharged species, and to charged species under conditions of high ionic strength. In these cases, the soft interactions can be treated in the Bragg–Williams approximation as relatively small perturbations on the hard-core potential.

(i) *Hard-core interactions*

Onsager (1949) was the first to consider the symmetry breaking effects of the excluded volume of asymmetric particles. Using a truncated density expansion of the free energy, he showed that excluded volume alone can cause an entropy-driven alignment transition for rods of sufficient axial ratio. Gelbart and co-workers have made use of this second virial treatment of excluded volume to describe the orientational ordering of self-assembling cylindrical micelles when aggregation is strong, and the aggregates are very much longer than they are wide, so that the transition occurs at concentrations low enough that three body and higher order terms are unimportant.

For higher concentrations, Gelbart and co-workers have used a 'y-expansion' (Barboy & Gelbart 1979, 1980; Gelbart *et al.* 1984; Gelbart & Barboy 1980). This approach is similar in form to the virial expansion, but instead of expanding the free energy in powers of the density of n-mers, ρ_n, one uses

$$y_n = \rho_n/(1.0-v_\mathrm{p}), \tag{2.4}$$

where v_p is the volume fraction of surfactant. The coefficients in the y-expansion are determined by successively expanding the lowest order terms in powers of ρ_n and matching the coefficients to those in the corresponding terms of the density expansion. Gelbart & Barboy (1980) find good agreement between their y-expansion (taken to third order for the free energy) and other methods, such as Percus–Yevick, scaled-particle, and Monte-Carlo, for a number of cases.

Herzfeld and co-workers have used closed-form expressions for the excluded volume contribution to the free energy, rather than density or y-expansions. Closed-form expressions can be derived using lattice combinatorics or scaled particle theory. An extension of the traditional lattice model of DiMarzio (1961) to accommodate arbitrary polydispersity in particle lengths and widths (Herzfeld 1982), has been applied to surfactant micelles (Taylor & Herzfeld 1991*a*) and protein fibres (Herzfeld

PHILOSOPHICAL TRANSACTIONS OF THE ROYAL SOCIETY A MATHEMATICAL, PHYSICAL & ENGINEERING SCIENCES

& Taylor 1988; Hentschke & Herzfeld 1989*b*). Although this lattice theory improves upon the second order virial treatment, a more accurate closed-form expression for the excluded volume contribution to the free energy is obtained by scaled particle theory. This approach makes use of the fact that the work of inserting a test particle into a solution of particles is known in the limiting cases in which the test particle is so small that it can interact with only one other particle (a straightforward two-body problem) and so large that insertion simply involves the PV work of making a macroscopic hole. Fortunately, it has been found that interpolation between these extremes, by scaling the dimensions of the test particle, provides results that agree well with Monte Carlo calculations (Taylor *et al.* 1989*b*; Hentschke *et al.* 1989; Taylor 1991*a*) and experimental results (Kubo & Ogino 1979; Kubo 1981). The scaled particle free energy has been given for polydisperse spherocylinders by Cotter & Wacker (1978) and for polydisperse spheroplatelets by Taylor (1991*b*). This treatment of excluded volume has been applied to several self-assembling systems (Taylor & Herzfeld 1990, 1991*a*; Hentschke & Herzfeld 1990*a*, 1991).

The above treatments of excluded volume apply to translationally disordered systems. However, self-assembling systems often form translationally ordered phases. If a cell model is used for the d translationally ordered dimensions (1 for lamellar phases, 2 for columnar phases and 3 for crystalline phases), then these dimensions are decoupled from the $3-d$ translationally disordered dimensions which can then be treated using a $(3-d)$-dimensional version of the fluid statistical treatments (Taylor *et al.* 1989*b*). Thus, translationally ordered phases of monodisperse particles of various shapes have been treated by combining d-dimensional cell models with $(3-d)$-dimensional scaled particle theory (Hentschke *et al.* 1989; Taylor & Herzfeld 1991*b*) or $(3-d)$-dimensional y-expansions (Sharlow *et al.* 1993). In self-assembling systems, the polydispersity of the particles suppresses some forms of positional ordering. However, the lamellar phases that occur in disk-forming systems and the columnar phases that occur in rod-forming systems can be treated by the above construction (Taylor & Herzfeld 1991*a*).

(ii) *Soft interactions*

Soft repulsions have two effects. The first, pointed out by Onsager (1949), may be viewed as an effective increase in the hard-core diameter of the particles. The second is an effective torque opposing the alignment of the particles (Stroobants *et al.* 1986; Hentschke & Herzfeld 1989*a*): two particles that are parallel and close enough to interact will have a higher free energy than two particles that are perpendicular at the same distance. (This is in contrast to the hard-core contribution to the free energy which is infinite when two particles interpenetrate, whether they are parallel or perpendicular.) Hentschke & Herzfeld (1989*a*) and Taylor & Herzfeld (1990, 1991*a*) have used a step potential to model soft-interactions: the potential has a constant value J (in units of kT) from the edge of the particle to a distance ζ beyond the particle edge, where it then drops to zero. With a positive value of J, this simple potential provides the main effect of soft repulsions by penalizing the shortest distances between particles and introducing the effective torque discussed above. Further, a sum of such step potentials (positive and/or negative) could be used to describe soft-interactions of any form.

(*d*) *Equilibrium state*

The equilibrium particle length and orientation distribution, $c(n, \Omega)$, is that which minimizes the free energy of the system. Using the expressions for the free energy, f, described above, we perform the functional derivative:

$$\left.\frac{\delta(f[c(n,\Omega)]-\chi\nu)}{\delta c(n',\Omega')}\right|_{V,T} = 0, \tag{2.5}$$

where ν is the volume fraction of solute present and χ is the Lagrange multiplier conjugate to the condition that

$$\nu = b_1 \int nc(n,\Omega)\,\mathrm{d}n\,\mathrm{d}\Omega, \tag{2.6}$$

where b_1 is the volume of a monomer. χ is also the difference between the chemical potentials of the solute and the solvent:

$$\chi = \mu_s - \mu_*. \tag{2.7}$$

There are two approaches to the calculus of variations. In the canonical approach (closed system) ν is fixed and χ is chosen such that the resulting $c(n, \Omega)$ gives the correct solute volume fraction. In the grand canonical approach (open system) χ is fixed and the resulting $c(n, \Omega)$ determines ν (Herzfeld 1988). Either way, a nonlinear integral equation for $c(n, \Omega)$ is obtained.

In solving for $c(n, \Omega)$ recourse to approximate or numerical methods is generally necessary and two approaches have been taken. McMullen *et al.* (1985) used an expansion in terms of the Legendre polynomials. Although exact, in principle, this method converges slowly for well aligned systems. Herzfeld and co-workers restricted the particles to three mutually orthogonal orientations (Taylor & Herzfeld 1991*a*; Hentschke & Herzfeld 1991). The tendency of this approximation to overestimate the orientational order of the system is less of a liability than might be expected. Onsager (1949) showed for monodisperse particles, that the nematic phases should be well aligned. This is in agreement with experimental studies of TMV in aqueous solution, in which it was found that the order parameter ($\langle P_2(\cos\otimes)\rangle$) is about 0.77 at the isotropic-nematic transition and increases rapidly to about 0.95 with increasing solute concentration (Oldenbourg *et al.* 1988). This cooperativity is accentuated in self-assembling systems where alignment is coupled to aggregate growth. In calculations for self-assembling proteins, Hentschke & Herzfeld (1989*b*) found that results were not changed dramatically by generalizing their model to allow a continuum of orientations.

3. Ordinary surfactants

Ordinarily surfactants comprise a polar (possibly ionic) hydrophilic head group and a flexible hydrophobic tail. At a critical concentration (CMC) the amphiphiles self-assemble into micelles. The surface-to-volume ratio of the micelle is restricted by the relation between the volume of the sequestered hydrophobic part of the molecule and the preferred packing of the head groups on the surface. For the micelles to grow with increasing surfactant concentration, while maintaining the necessary surface-

PHILOSOPHICAL TRANSACTIONS OF THE ROYAL SOCIETY A MATHEMATICAL, PHYSICAL & ENGINEERING SCIENCES

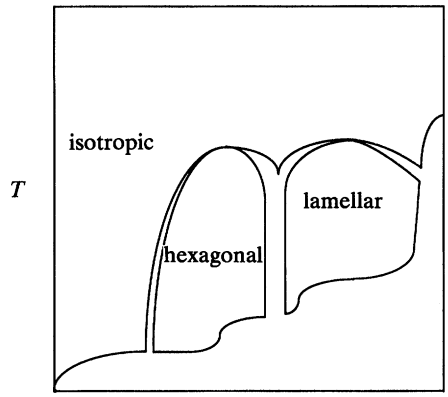

Figure 1. Schematic phase diagram for ordinary surfactants.

to-volume ratio, spherical symmetry must be broken (Tanford 1973). In proportions depending on the preferred surface curvature, growth may occur in one dimension, to form a rod-like micelle, and two dimensions, to form a plate-like micelle. The asymmetry of these aggregates can then induce various forms of long range order, including nematic, lamellar, hexagonal and cubic symmetries (Sonin 1987; Tiddy 1980). A typical phase diagram is shown schematically in figure 1. Interestingly, the nematic phase does not occur very often and then only in conjunction with salts or alcohols. It was widely believed, until relatively recently, that the role of the alcohol or salt was to prevent the growth of the aggregates into infinite rods or bilayers. However, X-ray data suggest that surfactant micelles are finite even in the hexagonal phase (Amaral *et al.* 1992). Moreover, as we will discuss in the next sections, Boden *et al.* (1987*a*) have recently shown that the behaviour of ordinary surfactants in the presence of alcohol or salt can be mimicked by self-assembling molecules that can form only rod-like or disc-like aggregates. This suggests that the effect of alcohol or salt on ordinary surfactants is to modify the relative stabilities of different micelle structures.

McMullen *et al.* (1985) have modelled micellar solutions with a second virial treatment of excluded volume and an explicit accounting of the size dependence of the translational and rotational contributions to the single particle partition functions. An interesting feature of the model is the description of the free energy of association in terms of the 'interfacial energy per unit area' at the surfactant-water interface, γ; the surface area per head group, a_0; the length of the hydrocarbon tail, l; and the volume of the surfactant molecule, v_0. These workers find a coupling between orientation and growth, much like that found by Herzfeld & Briehl (1981). An explosion of the length of the aggregates due to this coupling is prevented by the entropy of mixing contribution to the free energy. McMullen *et al.* also find that at the isotropic-nematic transition

$$\rho \bar{L}^2 D = \text{const.}, \tag{3.1}$$

where ρ is the number density of aggregates, $\bar{L}$ is the average aggregate length, and D is the aggregate diameter. This relation is analogous to the one obtained previously by Onsager (1949) and Flory (1956) for monodisperse rods. The effect of excluded volume on micelle growth in the isotropic phase was also examined more carefully

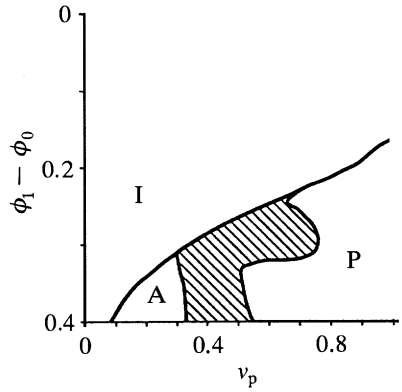

Figure 2. Calculated phase diagram for a model micellar system with $\phi_2 = \phi_1$ (Taylor *et al.* 1989*a*). I, isotropic phase; A, axial anisotropic phase; P, planar anisotropic phase. Shaded areas denote regions of phase coexistence.

using the y-expansion (Gelbart *et al.* 1984). It was found that excluded volume interactions enhanced the average aggregation number at mole fractions above 10^{-2} in the system that was studied.

To more fully understand the richness of surfactant phase diagrams, it is necessary to take account of the possibility of biaxial micelle growth. Taylor *et al.* (1989*a*) have performed calculations for self-assembling molecules that can form a polydisperse collection of biaxial particles, ranging from rods to plates. Through the relative values of ϕ_0, ϕ_1 and ϕ_2 (see §2*a*), the phenomenological free energy of aggregation controls the competition between the formation of new aggregates, the growth of aggregates into rods, and the growth of rods into plates. As shown in figure 2, it was found that excluded volume, described by lattice statistics, was sufficient to induce the experimentally observed variations in micelle shapes and orientational ordering with increasing concentration. In particular, when rod-like and plate-like micelle growth is equally favoured at the molecular level ($\phi_1 = \phi_2$), packing constraints induce a morphological rearrangement of the surfactant molecules from aligned rod-like micelles to aligned plate-like micelles, with increasing concentration. Although this succession of orientational symmetries agrees well with experiment, the comparison with experiment is not yet complete because the lattice theory did not include positionally ordered phases, against which the nematic phases might be unstable at higher concentrations.

4. Stacking polyaromatics (chromonics)

The complexity of the phase behaviour typical of surfactant solutions is due to the polymorphism of the micelles: for many surfactants the difference in stability between rod-like and disc-like micelles is relatively small, and packing constraints can tip the balance. In limiting cases, where either rod-like or plate-like aggregation is strongly preferred, the phase behaviour is simpler. In this section we discuss polyaromatic molecules which form exclusively rod-like aggregates. (This geometry also applies to the fibre forming proteins discussed in §6.) In §5 we will discuss rigid surfactants, and analogues, that form only disc-like aggregates. In all of these cases, the restriction to one aggregate geometry simplifies the phase diagram and expands the region of stability of nematic phases.

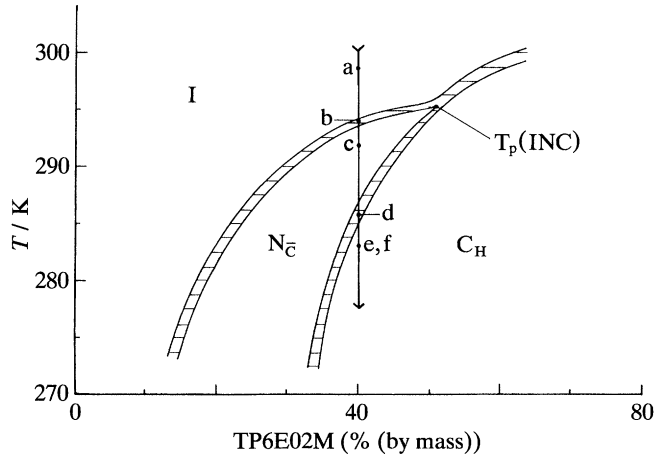

Figure 3. Phase diagram of Boden *et al.* (1986*a*) for TP6E02M/H_2O. I, isotropic phase; N_C^-, nematic phase with cylindrical micelles; C_H, hexagonal columnar phase; T_p(INC), isotropic-nematic-columnar triple point. Horizontal tie lines connect coexisting phases.

Lyotropic nematic and hexagonal mesophases are formed by a variety of polyaromatic dye and drug molecules that stack reversibly in cod-like aggregates (Vasilevskaya *et al.* 1989; Attwood *et al.* 1990; Perahia *et al.* 1991; and references therein). Boden *et al.* (1986*a*, *b*) have synthesized discoid molecules comprising a polyaromatic core surrounded by pendant hydrophilic side chains: 2, 3, 6, 7, 10, 11-hexa-(1,4,7-trioxaoctyl)-triphenylene (abbreviated TP6E02M). These amphiphiles can aggregate only by stacking on top of each other. The resulting aggregates are rod-like and the temperature dependence of the phase behaviour reflects the variation of the strength of aggregation with temperature. Here we are interested in transitions near room temperature. As shown in figure 3, there is an isotropic phase at low concentrations and a columnar phase at high concentrations. (A crystalline phase at still higher concentrations is not shown in figure 3.) At the low end of the temperature scale, a nematic phase intervenes between the isotropic and columnar phases. As the temperature increases, the isotropic-nematic transition is shifted to higher concentrations. The nematic-columnar transition is also shifted to higher concentrations, but relatively weakly. As a result, there is a triple point, T_p(INC), at about 295 K, above which the nematic phase disappears, leaving a direct isotropic-columnar transition. All these transitions are first-order, although the coexistence régimes are generally not very wide (Boden *et al.* 1986*a*, 1987*a*).

Taylor & Herzfeld (1990, 1991*a*) have modelled the polyaromatic system described above with a population of spherical monomers of diameter a and spherocylindrical aggregates of the same diameter. In this model, a spherocylinder assembled out of n monomers occupies the same volume as n monomers (i.e. no solvent is incorporated in the aggregates). A phenomenological free energy of aggregation was used which assumes that all contacts between monomers are identical. Excluded volume was treated by a combination of a cell model for translationally ordered dimensions and scaled particle theory for translationally disordered dimensions. The soft, short-range repulsive interactions were modelled by a step potential surrounding the particles and treated in the Bragg–Williams approximation (i.e. assuming negligible short-range order). The particle orientations were restricted to three mutually orthogonal axes.

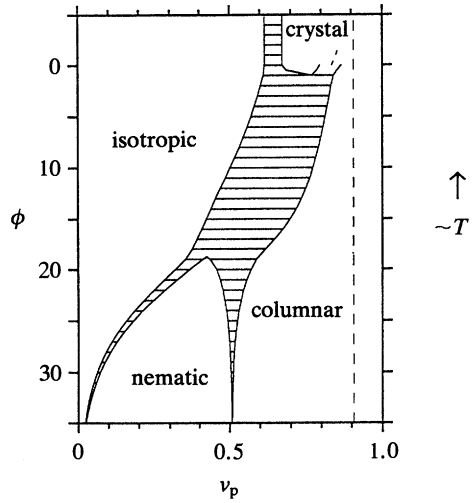

Figure 4. Calculated phase diagram for a system forming rod-like aggregates of diameter a with $aJ = 1.0$ and $\zeta/a = 0.1$ (Taylor & Herzfeld 1991*a*). Horizontal tie lines connect coexisting phases, while the vertical dashed line indicates the hard-rod close-packing limit. The dotted line indicates the crystal-columnar free-energy crossover, when the phase boundaries could not be found due to numerical problems.

The calculated phase diagram is shown in figure 4. To compare these results to the experimental data presented in figure 3, it is necessary to assume that ϕ, the free energy of contacts per monomer in units of kT, decreases with increasing temperature (i.e. that the enthalpy for *forming* contacts is positive). It is also assumed as a practical matter that J, the strength of the soft-repulsions in units of kT, is essentially constant. It is seen that the topology of the theoretical phase diagram is very similar to that of the experimental phase diagram, including the occurrence of a triple point where the isotropic, nematic and columnar phases coexist. Calculated values for the average aggregation number were also comparable to those found experimentally by Boden *et al.* (1986*b*, 1987*a*).

The above described model has been extended to consider the effects of adding a non-aggregating solute (B) to a solution of a linearly aggregating solute (A) (Madden & Herzfeld 1992*a*). The diameters of A and B need not be equal, but we discuss only that case here. If no B is present, the free energy expression is the same as that of Taylor & Herzfeld (1990). Species B contributes to the free energy through the excluded volume and the mixing terms in a manner analogous to monomers of A. The resulting ternary phase diagram is shown in figure 5 for $\phi = 21$. The previously calculated phase behaviour of the binary system of aggregating solute (A) and solvent (*) is found along the left leg of the diagram. Addition of species B in small amounts has little effect. The modest broadening of the isotropic-nematic and nematic-columnar coexistence regions reflects the difficulty of packing spherical monomers of B among parallel rod-like aggregates of A. The difficulty is greater at higher concentrations, and therefore influences the nematic-columnar transition more strongly than the isotropic-nematic transition. As more B is added the nematic phase disappears and a direct isotropic-columnar transition occurs with a very wide coexistence régime. The isotropic side of the coexistence régime is relatively dilute and depleted of the aggregating species while the columnar side is very dense and is enriched in the aggregating species. There is also a three phase region, in which

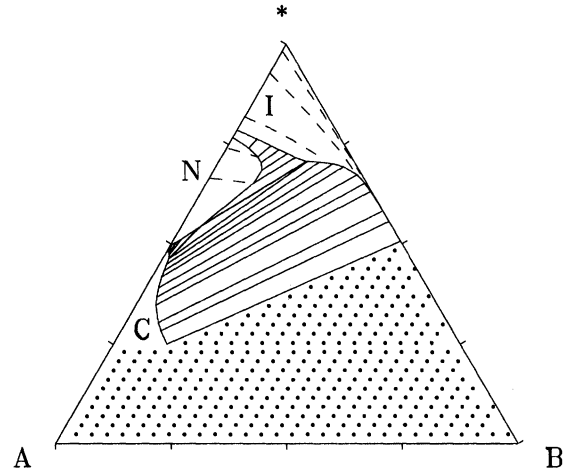

Figure 5. Calculated ternary phase diagram from Madden & Herzfeld (1992*a*) for a system comprising reversibly assembled spherocylindrical aggregates (A), non-aggregating spherical monomers (B), and solvent (*). The model parameters are identical to those of fig. 4 with $\phi = 21$. I, isotropic phase; *N*, nematic phase; *C*, columnar phase. Dashed lines indicate contours for average aggregation numbers (starting at the top) $10^{0.25}$, $10^{0.5}$, $10^{0.75}$, $10^{1.0}$ and $10^{1.25}$. The stippled region was numerically intractable.

isotropic, nematic and columnar phases coexist with very different compositions. Included in the diagram are average aggregation contours. In the ideal case that interparticle interactions could be neglected (valid only at very low concentrations), these contours would run parallel to the right leg (as is the tendency for the low solute concentrations near the apex of the diagram).

5. Rigid surfactants

The relatively rigid non-ionic surfactant analogue

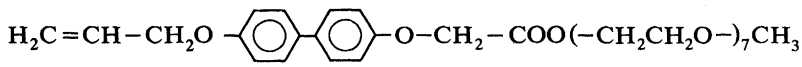

aggregates into discs and forms isotropic, nematic and lamellar phases in aqueous solution (Luhmann & Finkelmann 1986). In this system, over a narrow range of temperatures (7.5 °C to 23.4 °C), the nematic phase intervenes between a more dilute isotropic phase and a more concentrated lamellar phase. At higher temperatures, a direct isotropic-lamellar transition occurs. In each case, the transition is first order.

Boden *et al.* have seen similar behaviour in aqueous solutions of cesium pentadecafluorooctanonate (CsPFO) (Boden *et al.* 1986*c*, 1987*b*, 1989, 1992; Boden & Jolley 1992) and ammonium pentadecafluorooctanonate (APFO) (Boden *et al.* 1990). As APFO and CsPFO have qualitatively similar phase diagrams, only CsPFO is discussed here. CsPFO has a relatively rigid hydrophobic chain and a cation that has a low hydration energy. As a consequence, this amphiphile can only assemble into discs or bilayers. The resulting phase diagram, shown in figure 6 (Boden *et al.* 1989), is similar to that in figure 3, except that the positionally ordered phase at high concentrations is lamellar rather than columnar. As in figure 3, the nematic phase, which intervenes between the more dilute isotropic phase and the more concentrated positionally ordered phase at low temperatures, is gradually squeezed out with increasing temperature. Again, there is a triple point where the isotropic and

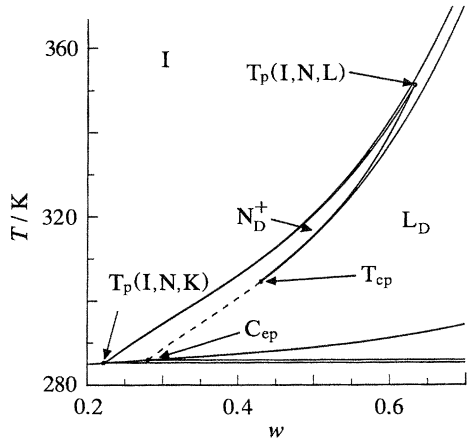

Figure 6. Phase diagram for CsPFO/H_2O (Boden *et al.* 1989). I, isotropic phase; N_D^+, nematic phase with discoidal micelles; L_D, discotic lamellar phase; T_{cp}, a tricritical point; T_p(I, N, L), the isotropic–nematic–lamellar triple point.

positionally ordered phases both coexist with the nematic phase, and above which a direct transition occurs between the isotropic and the positionally ordered phases. Based on X-ray diffraction measurements, Boden *et al.* (1986*c*) concluded that the lamellar phase consists of discrete discoid micelles. Photinos & Saupe (1990) subsequently argued, relying on density measurements with a vibrating densitometer and the slow relaxation time of the system, that the nematic-lamellar phase transition represents a change in the micellar structure to continuous lamellae. However, Boden & Jolley (1992) have shown that these results are not reproduced with density measurements using a classical dilatometer and make a convincing case for discrete discoid micelles in the lamellar phase.

Amphiphiles that aggregate exclusively into discs have been modelled by Taylor & Herzfeld (1991*a*). The aggregates in this work were right cylindrical discs of height a, and the monomers were right cylinders of height a and diameter a. The particles were restricted to three mutually orthogonal orientations. The phenomenological free energy of aggregation assigned a free energy ϕ for each monomer added to a disc. Again, excluded volume was treated by a combination of a cell model for positionally ordered dimensions and scaled particle theory for positionally disordered dimensions. The soft repulsive interactions were modelled by a step potential of height J and thickness ζ around the discs, and treated in the Bragg–Williams approximation.

The calculated phase diagram is shown in figure 7. Note that there is no crystalline phase because a crystal of orientationally ordered right cylinders is never stable when compared to the other phases (M. P. Taylor, personal communication). For strong aggregation (large ϕ) one obtains an isotropic phase followed by a nematic phase at higher concentrations, and a smectic at still higher concentrations. As ϕ decreases, the width of the nematic phase decreases until the nematic phase disappears at an isotropic-nematic-smectic triple point. To compare the calculated phase diagram with the experimental results of Boden *et al.* shown in figure 6, one again makes the assumption that ϕ decreases with increasing T, and that J is approximately constant. We see that the topology of the two diagrams is similar. In particular, the theory reproduces the contraction of the nematic region, between the isotropic and lamellar phases, leading to a triple point with increasing temperature. The change of

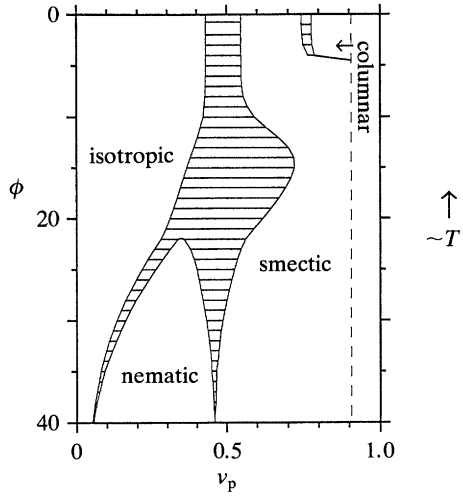

Figure 7. Calculated phase diagram for a system forming disc-like aggregates of thickness a with $a^2J = 0.2$ and $\zeta/a = 0.1$ (Taylor & Herzfeld 1991*a*). Horizontal tie lines connect coexisting phases and the vertical line indicates the hard-disc close-packing limit.

the nematic–smectic transition from first to second order with decreasing temperature, is not reproduced by the theory. This is because the cell model precludes a continuous transition to positional order. However the theory does find that the nematic–smectic transition becomes more weakly first order with increasing ϕ. Taylor and Herzfeld have also calculated average aggregation numbers and their results are similar to those from the X-ray diffraction work of Boden *et al.* (1986*c*). These results support the view that the lamellar phase comprises discrete micelles.

6. Proteins

The protein filaments that give structure and motility to cells are formed by the reversible assembly of monomeric proteins. Like the polyaromatic molecules discussed earlier, the proteins can only form rod-like aggregates (which are called polymers even though there are no covalent links between the monomers). Unlike the polyaromatics, but like ordinary surfactants, proteins form aggregates that are several monomers wide and a phenomenological description of assembly needs to distinguish between the formation of the minimum aggregates and the growth of these aggregates by further monomer addition.

The most thoroughly studied example of protein 'polymerization' is the pathological case of sickle-cell hemoglobin (HbS). The normal adult hemoglobin (HbA) monomer consists of four folded polypeptide chains (two α and two β) in a tetrahedral arrangement. The HbS monomer differs at one site on each of the two β chains: a negatively charged glutamic acid residue is replaced by a neutral and hydrophobic valine residue. This mutant valine fits into a hydrophobic pocket that is exposed on the β chain of a neighbouring Hb molecule when it is deoxygenated. The aggregate has 14 monomers in its cross-section and can grow indefinitely long.

Sedimentation is one of the most common experimental techniques used to study proteins, due to their relatively high density. In one application of this technique to HbS, a solution is centrifuged at high speed long enough for the high molecular weight polymers to be sedimented into the pellet (Hofrichter *et al.* 1976). The

PHILOSOPHICAL TRANSACTIONS OF THE ROYAL SOCIETY A MATHEMATICAL, PHYSICAL & ENGINEERING SCIENCES

concentration of deoxygenated hemoglobin left in the supernatant is then interpreted as the 'solubility' or 'saturating' concentration (c_{sat}), as if the hemoglobin had formed a macroscopic crystalline precipitate. This characterization is known as the two-phase model (Eaton & Hofrichter 1990). Another sedimentation technique makes use of the analytical ultracentrifuge (Briehl & Ewert 1973; Briehl 1978). First the polymer is removed from the solution by centrifugation at high speed, and then the centrifuge is decelerated to allow the solution of monomers to diffuse and the Schlieren peak to be measured. The results of this study are consistent with monomeric species at low concentrations, small isotropically oriented aggregates in a narrow range of intermediate concentrations, and an anisotropic phase at higher concentrations (Briehl 1978).

Osmotic pressure measurements provide a quantitative view of the thermodynamics of HbS behaviour, including aggregate growth and alignment. Prouty *et al.* (1985) dialysed solutions of deoxygenated HbS against solutions of inert polymers with known osmotic pressures and measured the corresponding equilibrium HbS concentrations. Data for 30 °C and 37 °C are shown in figure 8. At low concentrations the osmotic pressure is similar to that for HbA, indicating a solution of monomers. Above a temperature dependent concentration, the osmotic pressure deviates sharply from that for HbA. The insensitivity of the osmotic pressure to concentration in this region is suggestive of a first-order transition. However, microscopic birefringence studies indicate that the region of isotropic–nematic coexistence is narrower than the osmotic pressure plateau (P. R. Droupadi and co-workers, unpublished results). At still higher concentrations, the osmotic pressure increases again, but the increase is anomalously weak. Prouty *et al.* attributed these results to abrupt polymerization followed by gel compression. It should be noted that the measured osmotic pressures are inconsistent with the above mentioned two-phase model: this pseudo-condensation model predicts a constant osmotic pressure for all concentrations above that required for polymerization (analogous to the behaviour found for the non-polymerizing protein lysozyme, above its solubility limit).

Hentschke & Herzfeld (1990*a*, 1991) performed model calculations for the self-assembly of HbS, using scaled-particle theory to treat the excluded volume and a step potential for soft-repulsions. The known structure of the fibre was taken into account by including 14 monomers in the aggregate cross section and a variable amount of interstitial water. For the free energy of aggregation, a distinction was made between the free energy decrease per monomer (in units of kT) for contacts formed in the minimum aggregates (ϕ_0) against the contacts formed in extensions of the minimum aggregate into rods (ϕ_1). $\Delta\phi\,(=\phi_1-\phi_0)>0$ was chosen to reproduce the cooperativity of aggregation (i.e. the preference for addition to existing aggregates over the creation of new aggregates). Both the excluded volume and the free energy of aggregation were dependent on the solvent content of the polymer. The calculated osmotic pressure is shown in figure 8. We see that the model can account for the experimental data, including the appearance of aggregates at the high concentration end of the isotropic phase, the extension of the osmotic pressure plateau beyond a narrow isotropic-nematic coexistence region, and the nearly linear behaviour of the osmotic pressure at very high concentrations (which results from significant fibre dehydration under these conditions).

HbS often occurs *in vivo* mixed with appreciable amounts of other hemoglobins. Experimental results for such mixtures may depend on whether the hemoglobins are deoxygenated before or after mixing, since αβ units can be exchanged between

PHILOSOPHICAL TRANSACTIONS OF THE ROYAL SOCIETY A MATHEMATICAL, PHYSICAL & ENGINEERING SCIENCES

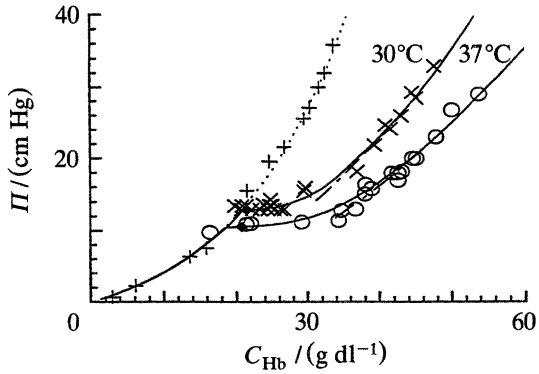

Figure 8. Osmotic pressure Π against concentration C_{Hb} for deoxygenated hemoglobin. Experimental data: HbS at 37 °C (○) and 30 °C (×) compared to the temperature insensitive behaviour of HbA (+) (Prouty *et al.* 1985). Theoretical calculations: osmotic pressure for HbA (····); osmotic pressure (——) and isotropic-nematic phase boundaries (◆) for HbS (Hentschke & Herzfeld 1991).

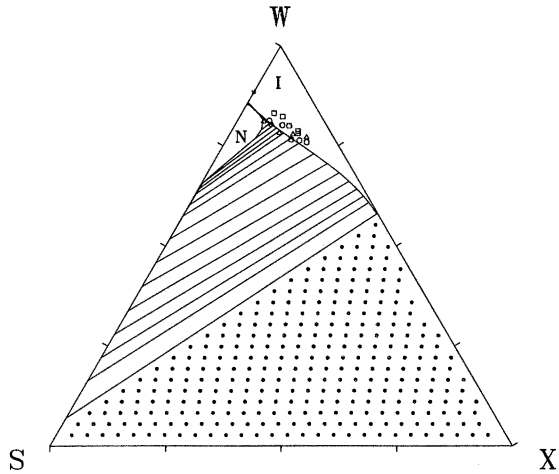

Figure 9. Calculated ternary phase diagram for HbS (S), water (W), and a hypothetical non-hybridizing and non-polymerizing HbX (X) (Madden & Herzfeld 1992*b*). The model parameters are identical to those for deoxy HbS at 37 °C in figure 8. I, isotropic phase; N, nematic phase. Tie lines connect coexisting phases. The stippled area was numerically intractable. Symbols: 'solubility' data from Benesch *et al.* (1980) for non-hybridized mixtures with HbA (□), HbA_2 (△) and HbF (○).

hemoglobins, to produce hybrid $(\alpha\beta)_2$ species, when the hemoglobins are oxygenated. The results of sedimentation experiments are reviewed by Eaton & Hofrichter (1990) and can be summarized as showing that (1) the onset of polymerization is shifted to higher *total* hemoglobin concentrations (though lower HbS concentrations) and (2) hybrid molecules can participate in polymerization. The osmotic pressure results for mixtures consist of one data set for hybridized HbA. The osmotic pressure plateau for this solution occurs at higher concentrations than for pure HbS, but the curve coincides with the monomeric osmotic pressure of pure HbA at concentrations below the plateau and the polymeric osmotic pressure of pure HbS at concentrations above the plateau (Prouty *et al.* 1985).

Madden & Herzfeld (1992*b*) have extended the above model of Hentschke & Herzfeld for HbS to a ternary system comprising HbS and a second hemoglobin

PHILOSOPHICAL TRANSACTIONS OF THE ROYAL SOCIETY A MATHEMATICAL, PHYSICAL & ENGINEERING SCIENCES

(HbX) in water. Results are shown in figure 9 for the case in which there is no hybridization and HbX does not participate in polymerization. The left leg of the diagram represents the phase behaviour of the binary HbS system at 37 °C shown in figure 8. As HbX is added, the isotropic boundary moves to higher concentrations. Since the isotropic boundary closely follows the onset of polymerization these can be compared with the solubility results from sedimentation studies. The agreement is seen to be good considering that conditions used for the binary osmotic pressure experiments (from which the theoretical parameters were derived) and the conditions used for the ternary sedimentation studies were different. Addition of HbX beyond a certain point also has the effect of causing dramatic demixing similar to that seen in figure 5. Since it was assumed that HbX does not hybridize or polymerize, the theoretically predicted osmotic pressure curves do not join the curve for pure HbS at high concentrations. Work is underway to extend the theory to take hybridization and copolymerization into account, as is necessary to consider the published osmotic pressure experiments and the physiological behaviour of HbS.

7. Conclusions

We have examined the relation between the very rich phase behaviour of self-assembling systems and the many microscopic degrees of freedom of these systems. Ordinary surfactants have the most degrees of freedom because they can form both rod-shaped and disc-shaped micelles. The balance between different morphologies is influenced by inter-micelle packing constraints, as well as intra-micelle interactions. Thus, with varying concentrations and temperatures, one observes a variety of symmetries of long-range ordering. Orientational ordering varies from axial alignment of rod-like aggregates at moderately high concentrations, to planar alignment of disc-like aggregates at still higher concentrations. This rearrangement of micelle morphology and orientational ordering with concentration is adequately described by a lattice model of micellar solutions. At sufficiently high concentrations, orientational ordering may be accompanied by translational ordering, resulting in columnar (hexagonal) phases for rod-like aggregates and smectic (lamellar) phases for disc-like aggregates. This behaviour has been described for systems restricted to rod-like or disc-like assembly by combining a cell model for the translationally ordered dimensions with a scaled particle treatment of the translationally disordered dimensions. The treatment of translational order in surfactant systems capable of forming both rod-like and disc-like micelles remains to complete the picture for binary systems. The behaviour of ternary systems has only begun to be explored theoretically. However, it is already evident that packing constraints can induce dramatic demixing of aggregating and non-aggregating species.

Aggregate flexibility is the most important aspect of self-assembling systems that has not yet been treated theoretically. Khokhlov & Semenov (1981, 1982) have shown that for persistent flexible polymers, the length scales for excluded volume interactions and polymer bending are sufficiently different to allow the contributions of the two effects to the free energy to be treated separately. Their theory has been extended to higher concentrations, by replacing their second virial treatment of excluded volume with more rigorous treatments, and the results agree well with experimental data for solutions of monodisperse persistent flexible polymers (Hentschke 1990; Hentschke & Herzfeld 1990*b*; DuPre & Yang 1991). However, to apply this approach to self-assembling systems, it will be necessary to extend the

PHILOSOPHICAL TRANSACTIONS OF THE ROYAL SOCIETY A MATHEMATICAL, PHYSICAL & ENGINEERING SCIENCES

theory to allow for polydispersity, i.e. the simultaneous occurrence of aggregate lengths that vary from much shorter to much longer than the aggregate persistence length. Efforts along these lines are in progress.

We thank Neville Boden for suggesting that we write this review, and Mark Taylor and Jining Han for helpful discussions. T.L.M. was supported by NRSA HL08472.

References

Amaral, L. Q., Gulik, A., Itri, R. & Mariani, P. 1992 Micellar hexagonal phases in lyotropic liquid crystals. *Phys. Rev.* A **46**, 3548–3550.

Attwood, T. K., Lydon, J. E., Hall, C. & Tiddy, G. J. T. 1990 The distinction between chromonic and amphiphilic lyotropic mesophases. *Liquid Cryst.* **7**, 657–668.

Barboy, B. & Gelbart, W. M. 1979 Series representation of the equation of state for hard particle fluids. *J. chem. Phys.* **71**, 3053–3062.

Barboy, B. & Gelbart, W. M. 1980 Hard-particle fluids. II. General y-expansion-like descriptions. *J. statist. Phys.* **22**, 709–742.

Benesch, R. E., Edalji, R., Kwong, S. & Benesch, R. 1980 Solubilization of hemoglobin S by other hemoglobins. *Proc. U.S. natn. Acad. Sci.* **77**, 5130–5134.

Boden, N., Bushby, R. J., Hardy, C. & Sixl, F. 1986*a* Phase behavior and structure of a non-ionic discoidal amphiphile in water. *Chem. Phys. Lett.* **123**, 359–364.

Boden, N., Bushby, R. J., Ferris, L., Hardy, C. & Sixl, F. 1986*b* Designing new lyotropic amphiphilic mesogens to optimize the stability of nematic phases. *Liquid Cryst.* **2**, 109–125.

Boden, N., Corne, S. A., Holmes, M. C., Jackson, P. H., Parker, D. & Jolley, K. W. 1986*c* Order-disorder transitions in solutions of discoid micelles. *J. Phys., Paris* **47**, 2135–2144.

Boden, N., Bushby, R. J., Jolley, K. W., Holmes, M. C. & Sixl, F. 1987*a* Factors governing the stability of micellar nematic phases. *Molec. Cryst. Liquid Cryst.* **152**, 37–55.

Boden, N., Corne, S. A. & Jolley, K. W. 1987*b* Lyotropic mesomorphism of the cesium pentadecafluorooctanoate/water system: high-resolution phase diagram. *J. phys. Chem.* **91**, 4092–4105.

Boden, N., Jolley, K. W. & Smith, M. H. 1989 Location of the discotic-lamellar tricritical point and isotope effects in the caesium pentadecafluorooctanoate (CsPFO)/water system as established by ^{133}Cs N.M.R. spectroscopy. *Liquid Cryst.* **6**, 481–488.

Boden, N., Clements, J., Jolley, K. W., Parker, D. & Smith, M. H. 1990 Nematic-lamellar tricritical behavior and structure of the lamellar phase in the ammonium pentadecafluorooctanoate (APFO)/water system. *J. chem. Phys.* **93**, 9096–9105.

Boden, N., Edwards, P. J. B. & Jolley, K. W. 1992 Self-assembly and self-organization in micellar liquid crystals. In *Structure and dynamics of strongly interacting colloids and supramolecular aggregates in solution* (ed. S. Chen, J. S. Huang & P. Tartaglia), pp. 433–461. Kluwer.

Boden, N. & Jolley, K. W. 1992 Interpretation of density and conductivity measurements in the liquid-crystal phases of the cesium pentadecafluorooctanoate-water system and its implication for the structure of the lamellar phase. *Phys. Rev.* A **45**, 8751–8758.

Briehl, R. W. 1978 Gelation of sickle cell hemoglobin. IV. Phase transitions in hemoglobin S gels: separate measures of aggregation and solution-gel equilibrium. *J. molec. Biol.* **123**, 521–538.

Briehl, R. W. & Ewert, S. 1973 Effects of pH, 2,3-diphosphoglycerate and salts on gelation of sickle cell deoxyhemoglobin. *J. molec. Biol.* **80**, 445–458.

Cotter, M. A. & Wacker, D. C. 1978 Van der Waals theory of nematogenic solutions. I. Derivation of the general equations. *Phys. Rev.* A **18**, 2669–2675.

DiMarzio, E. 1961 Statistics of orientation effects in linear polymer molecules. *J. chem. Phys.* **35**, 658–669.

DuPre, D. B. & Yang, S. 1991 Liquid crystalline properties of solutions of persistent polymer chains. *J. chem. Phys.* **94**, 7466–7477.

Eaton, W. A. & Hofrichter, J. 1990 Sickle cell hemoglobin polymerization. *Adv. Protein Chem.* **40**, 63–280.

PHILOSOPHICAL TRANSACTIONS OF THE ROYAL SOCIETY A MATHEMATICAL, PHYSICAL & ENGINEERING SCIENCES

Flory, P. J. 1956 Phase equilibria in solutions of rod-like particles. *Proc. R. Soc. Lond.* A **234**, 73–89.

Gelbart, W. M. & Barboy, B. 1980 A van der Waals picture of the isotropic-nematic liquid crystal phase transition. *Acc. Chem. Res.* **13**, 290–296.

Gelbart, W. M., Ben-Shaul, A., McMullen, W. E. & Masters, A. 1984 Micellar growth due to interaggregate interactions. *J. phys. Chem.* **88**, 861–866.

Gelbart, W. M., McMullen, W. E. & Ben-Shaul, A. 1986 Theory of micellar stability in isotropic and nematic phases. *Molec. Cryst. Liquid Cryst.* **132**, 325–337.

Hentschke, R. 1990 Equation of state for persistent-flexible-liquid-crystal polymers. Comparison with poly(γ-benzyl-L-glutamate) in dimethylformamide. *Macromolecules* **23**, 1192–1196.

Hentschke, R., Taylor, M. P. & Herzfeld, J. 1989 Equation of state for parallel hard spherocylinders. *Phys. Rev.* A **40**, 1678–1680.

Hentschke, R. & Herzfeld, J. 1989*a* Soft repulsions in a lattice model for liquid crystalline order in self-assembling systems. *J. chem. Phys.* **91**, 7308–7309.

Hentschke, R. & Herzfeld, J. 1989*b* Nematic behavior of reversibly polymerizing proteins. *J. chem. Phys.* **90**, 5094–5101.

Hentschke, R. & Herzfeld, J. 1990*a* Dehydration of protein polymers in concentrated nematic solutions. *Mater. Res. Soc. Proc.* **177**, 305–310.

Hentschke, R. & Herzfeld, J. 1990*b* Simple theory for persistent-flexible liquid crystal polymers beyond the second virial approximation. *Mater. Res. Soc. Proc.* **177**, 323–328.

Hentschke, R. & Herzfeld, J. 1991 Theory of nematic order with aggregate dehydration for reversibly assembling proteins in concentrated solutions: Application to sickle-cell hemoglobin polymers. *Phys. Rev.* A **43**, 7019–7030.

Herzfeld, J. 1982 Lattice statistics for highly heterogeneous populations of rigid rectangular particles. *J. chem. Phys.* **76**, 4185–4190.

Herzfeld, J. 1988 Liquid crystalline order in self-assembling systems: orientation dependence of the particle size distribution. *J. chem. Phys.* **88**, 2776–2779.

Herzfeld, J. & Briehl, R. 1981 Phase behavior of reversibly polymerizing systems with narrow length distributions. *Macromolecules* **14**, 397–404.

Herzfeld, J. & Taylor, M. P. 1988 Unexpected critical points in the nematic behavior of a reversibly polymerizing system. *J. chem. Phys.* **88**, 2780–2787.

Hofrichter, J., Ross, P. D. & Eaton, W. A. 1976 Supersaturation in sickle cell hemoglobin solutions. *Proc. U.S. natn. Acad. Sci.* **73**, 3035–3039.

Khokhlov, A. R. & Semenov, A. N. 1981 Liquid-crystalline ordering in the solution of long persistent chains. *Physica* **108**A, 546–556.

Khokhlov, A. R. & Semenov, A. N. 1982 Liquid-crystalline ordering in the solution of partially flexible macromolecules. *Physica* **112**A, 605–614.

Kubo, K. & Ogino, K. 1979 Comparison of osmotic pressure for the poly(γ-benzyl-L-glutamate) solutions with the theories for a system of hard spherocylinders. *Molec. Cryst. Liquid Cryst.* **53**, 207–228.

Kubo, K. 1981 Thermodynamic properties of poly(γ-benzyl-L-glutamate) solutions over entire concentration range. *Molec. Cryst. Liquid Cryst.* **74**, 71–87.

Luhmann, B. & Finkelmann, H. 1986 A lyotropic nematic phase of lamellar micelles (N_L) obtained by a non-ionic surfactant in aqueous solution. *Colloid Polymer Sci.* **264**, 189–192.

Madden, T. L. & Herzfeld, J. 1992*a* Exclusion of spherical particles from the nematic phase of reversibly assembled rod-like particles. *Mater. Res. Soc. Proc.* **248**, 95–101.

Madden, T. L. & Herzfeld, J. 1992*b* Solubilization of sickle-cell hemoglobin polymers by fetal hemoglobin. *FASEB J.* **6**, A58.

McMullen, W. E., Gelbart, W. M. & Ben-Shaul, A. 1984*a* Translational and rotational contributions to the size of micelles in dilute surfactant solutions. *J. phys. Chem.* **88**, 6649–6654.

McMullen, W. E., Ben-Shaul, A. & Gelbart, W. M. 1984*b* Rod/disk coexistence in dilute soap solutions. *J. Colloid Interface Sci.* **98**, 523–536.

McMullen, W. E., Gelbart, W. M. & Ben-Shaul, A. 1985 Isotropic–nematic transition in micellized solutions. *J. chem. Phys.* **82**, 5616–5623.

PHILOSOPHICAL TRANSACTIONS OF THE ROYAL SOCIETY A MATHEMATICAL, PHYSICAL & ENGINEERING SCIENCES

Oldenbourg, R., Wen, X., Meyer, R. B. & Caspar, D. L. D. 1988 Orientational distribution function in nematic tobacco-mosaic-virus liquid crystals measured by X-ray diffraction. *Phys. Rev. Lett.* **61**, 1851–1854.

Onsager, L. 1949 The effects of shape on the interaction of colloidal particles. *Ann. N.Y. Acad. Sci.* **51**, 627–660.

Perahia, D., Wachtel, E. J. & Luz, Z. 1991 NMR and X-ray studies of the chromonic lyomesophases formed by some xanthone derivatives. *Liquid Cryst.* **9**, 479–492.

Photinos, P. & Saupe, A. 1990 Slow relaxation effects at the second-order nematic to lamellar smectic phase transition in micellar liquid crystals. *Phys. Rev.* A **41**, 954–959.

Prouty, M. S., Schechter, A. N. & Parsegian, V. A. 1985 Chemical potential measurements of deoxyhemoglobin S polymerization determination of the phase diagram of an assembling protein. *J. molec. Biol.* **184**, 517–528.

Sharlow, M. F., Ben-Shaul, A. & Gelbart, W. M. 1993 Layered and hexagonal states of aligned, hard disks vs. rods. (Submitted.)

Sonin, A. S. 1987 Lyotropic nematics. *Sov. Phys. Usp.* **30**, 875–896.

Stroobants, A., Lekkerkerker, H. N. W. & Odijk, Th. 1986 Effect of electrostatic interaction on the liquid crystal phase transition in solutions of rodlike polyelectrolytes. *Macromolecules* **19**, 2232–2238.

Tanford, C. 1973 *The hydrophobic effect: formation of micelles and biological membranes.* New York: John Wiley and Sons.

Taylor, M. P. 1991*a* Statistical mechanical models of liquid crystalline ordering in reversibly assembling lyotropic systems. Ph.D. thesis, Brandeis University, Waltham, Massachusetts, U.S.A.

Taylor, M. P. 1991*b* Excluded volume for polydisperse spheroplatelets. *Liquid Cryst.* **9**, 141–143.

Taylor, M. P., Berger, A. E. & Herzfeld, J. 1989*a* Theory of amphiphilic liquid crystals: Multiple phase transitions in a model micellar system. *J. chem. Phys.* **91**, 528–538.

Taylor, M. P., Hentschke, R. & Herzfeld, J. 1989*b* Theory of ordered phases in a system of parallel hard spherocylinders. *Phys. Rev. Lett.* **62**, 800–803.

Taylor, M. P. & Herzfeld, J. 1990 Phase diagram for reversibly-assembled rod-like aggregates: nematic, columnar and crystalline ordering. *Mater. Res. Soc. Proc.* **177**, 135–140.

Taylor, M. P. & Herzfeld, J. 1991*a* Shape anisotropy and ordered phases in reversibly assembling lyotropic systems. *Phys. Rev.* A **43**, 1892–1905.

Taylor, M. P. & Herzfeld, J. 1991*b* Nematic and smectic order in a fluid of biaxial hard particles. *Phys. Rev.* A **44**, 3742–3751.

Tiddy, G. J. T. 1980 Surfactant-water liquid crystal phases. *Phys. Rep.* **57**, 1–46.

Vasilevskaya, A. S., Generalova, E. V. & Sonin, A. S. 1989 Chromonic Mesophases. *Russ. chem. Rev.* **58**, 904–916.

PHILOSOPHICAL TRANSACTIONS OF THE ROYAL SOCIETY A MATHEMATICAL, PHYSICAL & ENGINEERING SCIENCES